Cell Reports Methods, Volume *1*

Supplemental information

A high-content platform for physiological profiling and unbiased classification of individual neurons

Daniel M. DuBreuil, Brenda M. Chiang, Kevin Zhu, Xiaofan Lai, Patrick Flynn, Yechiam Sapir, and Brian J. Wainger

Supplementary Figures 1-6

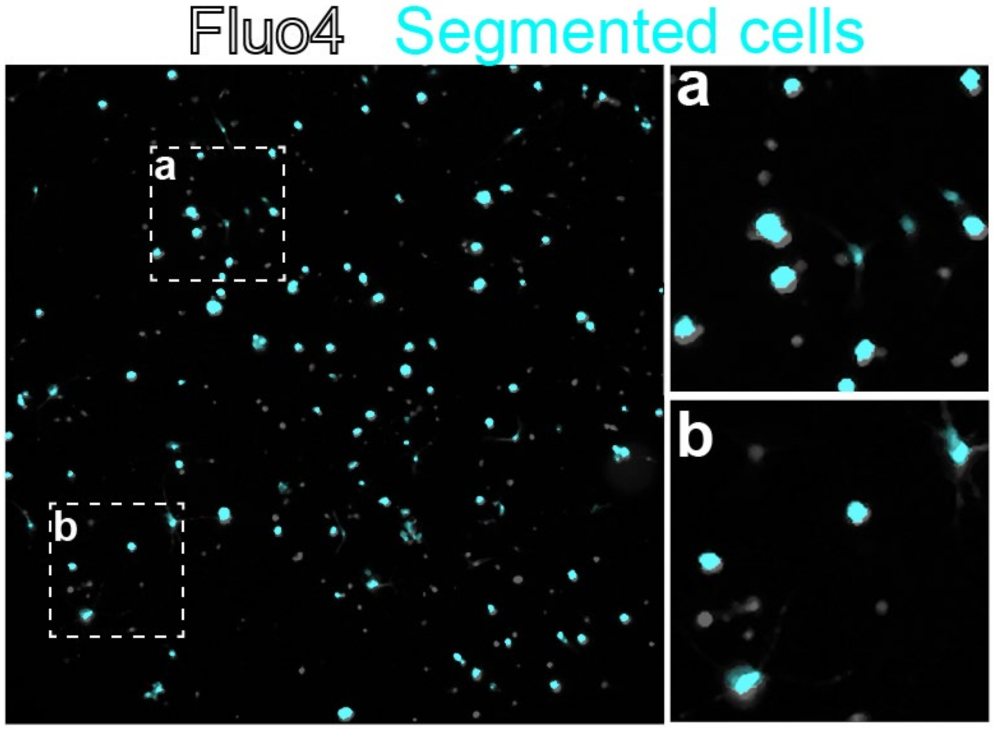

Supplementary Figure 1. Results of automated cell segmentation, Related to Figure 1**.** Example image of Fluo4 signal (white) and results of automated segmentation (cyan) for one well. Time-lapse image stacks of Fluo4 signal are projected into a single image using minimum pixel intensity to remove cells that move during imaging. The projection image is blurred using a gaussian filter and an automatic global threshold applied to identify objects.

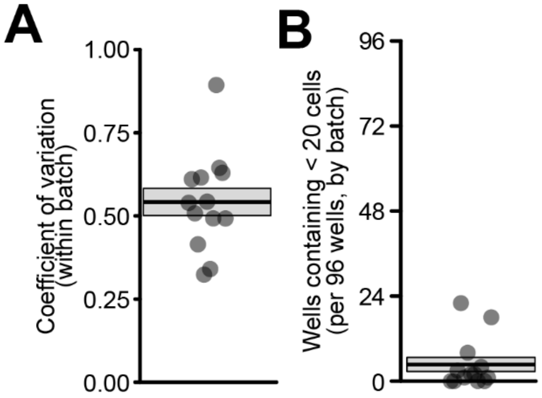

Supplementary Figure 2. Neurons are evenly distributed across individual plates with few low-density wells, Related to Figure 1**.**

A, Coefficient of variation within each plate (points), along with mean and SEM (box, 0.542 ± 0.041).

B, Wells per 96-well batch with fewer than 20 cells per well (points), along with mean and SEM (box, 4.7 ± 2.0 wells per 96-well batch).

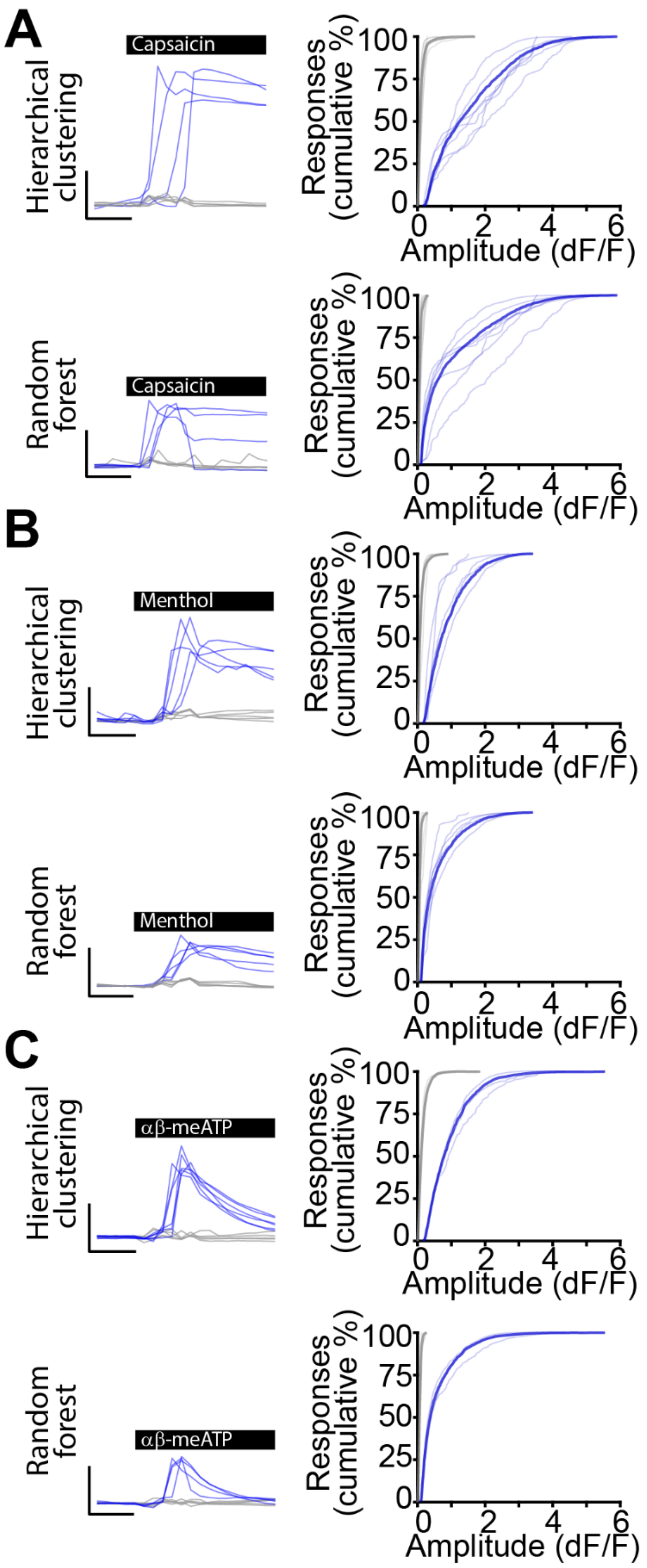

Supplementary Figure 3. Unbiased classification of responses to Trp and puringergic receptor agonists, Related to Figure 2**.** Classification of calcium responses following application of **A,** capsaicin**, B,** menthol**,** and **C,** meATP by hierarchical clustering (top) and random forest machine learning (bottom) approaches. Each panel shows example traces of calcium responses classified as positive (blue) and negative (grey) (left, scale bars 5 s and 0.5 dF/F) along with cumulative distributions of positive (blue) and negative (grey) response amplitudes (right).

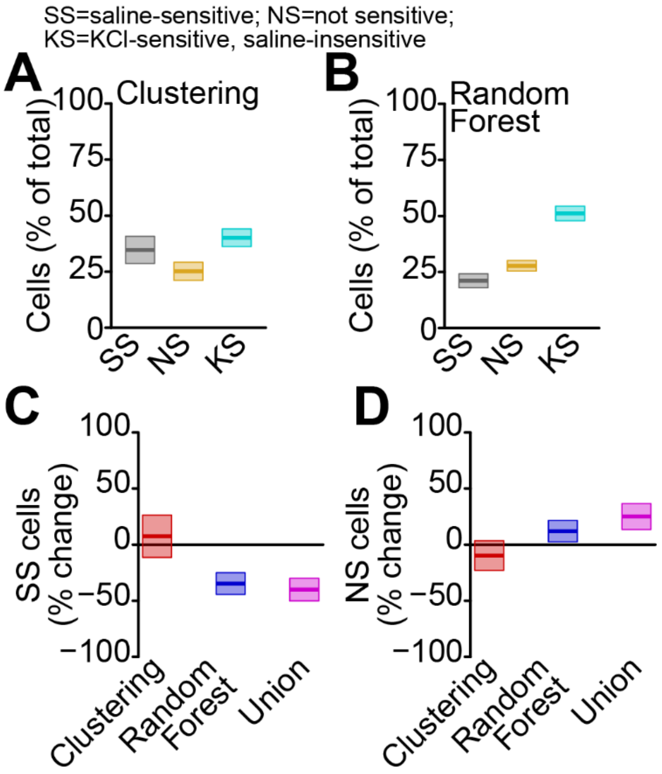

Supplementary Figure 4. Comparison of individual, unbiased approaches for quantification of cell types, Related to Figure 2**. A-B,** Percentage of cells classified as SS (grey), NS (orange), and KS (cyan) using hierarchical clustering (**A**) or random forest classifiers (**B**). **C-D,** Percent change from threshold-based analysis in percentage of SS cells (**C**) or NS cells (**D**) using hierarchical clustering (red) or random forest (blue) classifiers alone or the union of both approaches (magenta).

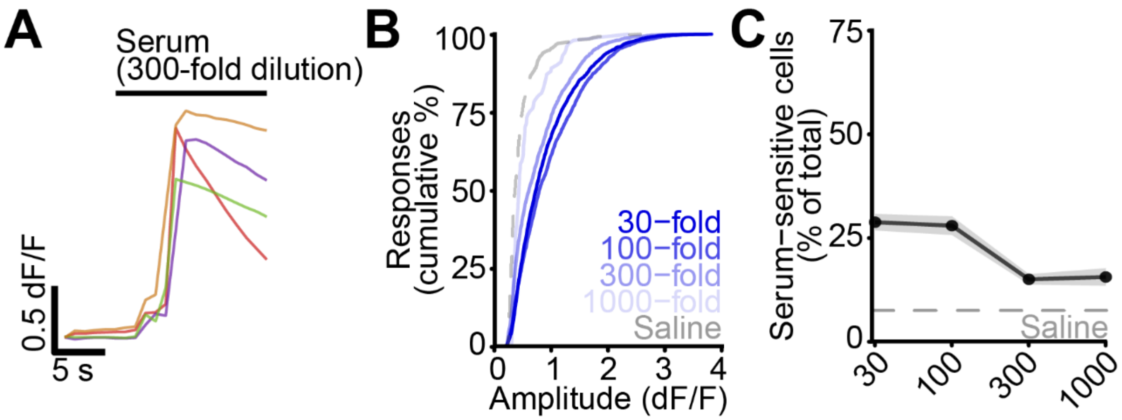

Supplementary Figure 5. Activation of primary mouse sensory neurons by human serum samples, Related to figure 5**.**

A, Example traces of positive responses to serum (300-fold dilution, colors indicate individual cells, scale bars 5 s and 0.5 dF/F).

B, Cumulative distributions of positive response amplitudes following stimulation by serum dilutions (as fold dilution, orange), along with meATP (dashed green line) and saline (dashed grey line). Analysis includes cells sensitive to initial saline stimulus.

C, Dose-response curve of sensory neuron activation by serum as mean (points/lines) and SEM (shaded area), along with saline-dependent activation (dashed line). Analysis includes cells sensitive to initial saline stimulus.

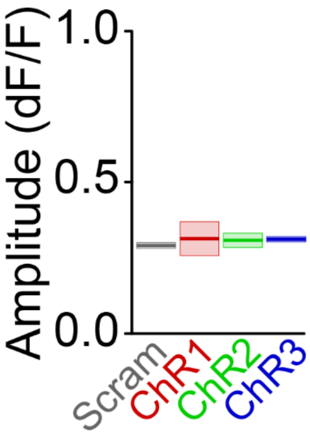

Supplementary Figure 6. Effect of ChR-targeting ASOs on amplitude of optogenetic responses, Related to Figure 6**.** Average response amplitude of positive responses following optical stimulation after seven-day treatment by ChR2-targeting ASOs (red, green, blue) or scrambled control ASO (grey) as mean and SEM.

Supplementary Tables 1-2

Accuracy [95% confidence interval]		Test batch									
		#1	#2	#3	#4	#5	#6	#7	#8	#9	#10
Training batch	#1		92.5 [92,92.9]	96.1 [95.9,96.3]	85.3 [84.5,86.1]	80.1 [79,81.1]	80.1 [79.4,80.8]	86 [85.5,86.6]	80.5 [79.6,81.4]	79.9 [79.4,80.3]	77.7 [77.2,78.2]
	#2	94.5 [94.2,94.7]		95.1 [94.9,95.4]	83.2 [82.3,84]	81.6 [80.6,82.5]	81.8 [81.1,82.5]	86.1 [85.5,86.6]	80.8 [79.9,81.7]	84.3 [83.9,84.7]	81.1 [80.6,81.6]
	#3	96.6 [96.4,96.8]	93.1 [92.7,93.5]		81.8 [80.9,82.6]	79.6 [78.6,80.6]	74.8 [74.1,75.6]	86.2 [85.7,86.7]	79.8 [78.8,80.7]	76.6 [76.1,77.1]	77.8 [77.3,78.3]
	#4	94.4 [94.2,94.7]	91 [90.5,91.5]	94.2 [93.9,94.4]		86.7 [85.8,87.6]	91.6 [91.1,92.1]	90.9 [90.5,91.3]	89.4 [88.7,90.1]	89.8 [89.4,90.1]	92.8 [92.5,93.1]
	#5	94.6 [94.3,94.8]	93.3 [92.8,93.7]	95.9 [95.6,96.1]	92.2 [91.6,92.8]		88.7 [88.1,89.2]	91.5 [91.1,91.9]	87.5 [86.7,88.2]	90.1 [89.7,90.4]	86.5 [86.1,86.9]
	#6	91.7 [91.4,92.1]	91 [90.5,91.5]	90.1 [89.7,90.4]	93.6 [93,94.1]	85.7 [84.8,86.6]		92.9 [92.5,93.2]	88.5 [87.7,89.2]	94.6 [94.3,94.8]	89.5 [89.1,89.9]
	#7	91.9 [91.6,92.2]	89.7 [89.1,90.2]	92.8 [92.5,93.1]	91.5 [90.9,92.1]	85.4 [84.4,86.2]	92.8 [92.4,93.3]		86.5 [85.7,87.2]	91.9 [91.6,92.2]	86.3 [85.8,86.7]
	#8	95.1 [94.8,95.3]	92 [91.5,92.4]	96.2 [95.9,96.4]	88.9 [88.2,89.6]	82.1 [81.1,83.1]	85.5 [84.9,86.2]	87.9 [87.4,88.4]		85.3 [84.9,85.7]	86 [85.6,86.4]
	#9	92.4 [92.1,92.7]	92.4 [91.9,92.8]	93.1 [92.8,93.4]	93.5 [93,94]	87 [86.1,87.8]	95.7 [95.3,96.1]	93.5 [93.1,93.9]	89.9 [89.2,90.5]		90.1 [89.7,90.5]
	#10	74 [73.5,74.6]	81.2 [80.5,81.9]	68.6 [68,69.1]	84.6 [83.8,85.4]	77.9 [76.9,79]	75.3 [74.5,76]	84.2 [83.6,84.7]	90.1 [89.4,90.7]	78.6 [78.2,79.1]	

Supplementary Table 1. Robust classification of responses across neuronal batches, Related to Figure 2**.** Accuracy and 95% confidence intervals for pairwise classification of individual test batches using random forest models trained on independent single batches. All accuracy values are statistically significant with $p < 5*10^{-100}$.

		Nociceptor Enrichment		DRG specificity		Effect of Injury		Agonist			
Gene	Class/Type	logFC	p-value	logFC	p-value	logFC	p-value	Name	Source	Dose	Ref (PMID)
Il13ra1	cytokine	2.6540	6.87E-07	-1.4900	3.35E-01	0.6329	1.42E-09	IL-13	Sigma	1 / 10 / 100 ng/mL	19383494
Il31ra	cytokine	3.3072	3.31E-07	4.4350	1.61E-09	0.0905	3.63E-01	IL-31	Sigma	0.1 / 1 / 10 ng/mL	24373353
Il6st	cytokine	0.9212	4.61E-07	2.9300	6.86E-02	0.0986	3.75E-01	IL-6	Sigma	0.1 / 1 / 10 ng/mL	32519575
Lifr	cytokine	0.5511	1.28E-04	3.6500	6.48E-03	0.0241	3.88E-01	LIF	Sigma	0.1 / 1 / 10 ng/mL	10380072
Gfra3	growth factor	3.2960	5.97E-08	4.0600	1.49E-62	0.4092	6.48E-04	GDNF	Life Tech	10 / 50 / 100 ng/mL	22704965
Ngfr	growth factor	0.8134	7.06E-04	7.9100	1.77E-48	-0.0094	8.63E-01	NGF	R&D	10 / 100 / 500 ng/mL	30211336
Ptgdr	lipid	2.7043	2.52E-07	2.0500	7.39E-36	0.0495	6.38E-01	AMG 853	Tocris	20 / 200 / 2000 nM	24900313
Ptgir	lipid	2.3355	1.20E-04	4.6800	8.02E-04	-0.2397	6.62E-04	Treprostinil	Tocris	2 / 20 / 200 nM	22480736
S1pr3	lipid	0.5829	2.60E-03	5.5000	5.38E-05	-0.0127	7.46E-01	CYM 5541	Tocris	0.1 / 1 / 10 µM	22971058
Lpar3	lipid	1.9022	1.55E-06	6.5600	1.69E-13	-0.1790	9.17E-02	1-Oleoyl LPA	Tocris	2 / 20 / 200 µM	15353230
Ptger3	lipid	1.7593	1.92E-07	1.2191	4.87E-01	0.0502	3.66E-01	Sulprostone	Tocris	5 / 50 / 500 ng/mL	17700719
Galr1	peptide	3.7567	1.85E-08	-0.0122	7.02E-01	-0.0169	5.74E-01	Galanin	Tocris	5 / 50 / 500 nM	19006083
Npy2r	peptide	4.0898	4.26E-09	4.6400	1.14E-06	0.2926	3.13E-03	YY (3-36)	Tocris	5 / 50 / 500 ng/mL	29157865
Sstr2	peptide	2.8811	2.07E-06	1.7200	7.23E-02	0.0528	1.77E-01	L-054,264	Tocris	5 / 50 / 500 nM	9632348
Cckbr	peptide	0.5116	1.05E-01	-0.4085	7.18E-01	2.8349	3.77E-12	Gastrin I	Tocris	5 / 50 / 500 ng/mL	8476056
F2rl2	peptide	2.4652	8.26E-07	3.2450	9.35E-11	-0.1263	7.52E-02	Thrombin	Tocris	0.5 / 5 / 50 µg/mL	11487506
Agtr1a	peptide	2.7214	2.58E-06	3.6800	5.69E-02	-0.0873	1.43E-01	Angiotensin II	Tocris	5 / 50 / 500 ng/mL	23255326
Ret	RTK	0.7972	5.73E-07	8.3500	2.46E-14	0.1147	1.46E-01	XIB-4035	Sigma	10 /100 / 1000 µM	12441171

Supplementary Table 2. Pool of metabotropic receptor agonists from *in silico* analysis of transcriptomic datasets, Related to Figure 4**.**